

# Analytical Methods

Accepted Manuscript



This is an *Accepted Manuscript*, which has been through the Royal Society of Chemistry peer review process and has been accepted for publication.

*Accepted Manuscripts* are published online shortly after acceptance, before technical editing, formatting and proof reading. Using this free service, authors can make their results available to the community, in citable form, before we publish the edited article. We will replace this *Accepted Manuscript* with the edited and formatted *Advance Article* as soon as it is available.

You can find more information about *Accepted Manuscripts* in the [Information for Authors](#).

Please note that technical editing may introduce minor changes to the text and/or graphics, which may alter content. The journal's standard [Terms & Conditions](#) and the [Ethical guidelines](#) still apply. In no event shall the Royal Society of Chemistry be held responsible for any errors or omissions in this *Accepted Manuscript* or any consequences arising from the use of any information it contains.

## ARTICLE

# Hybrid of non-selective quantum dots for simultaneous determination of TNT and 4-Nitrophenol using multivariate chemometrics methods

Cite this: DOI: 10.1039/x0xx00000x

Received 00th January 2012,  
Accepted 00th January 2012

DOI: 10.1039/x0xx00000x

www.rsc.org/

Ali Barati,<sup>a</sup> Mojtaba Shamsipur<sup>b</sup> and Hamid Abdollahi<sup>\*a</sup>,

Herein, we used the overall fluorescence of a nanohybrid fluorescence probe comprised of carbon quantum dots (CQDs) and CdTe QDs to pattern-based discrimination of different analytes using principal component analysis and also to simultaneous determination in a binary mixture of analytes using multivariate chemometrics methods such as partial least-squares (PLS) and artificial neural network (ANN). The fluorescence intensity of both QDs was quenched in the presence of six different nitro-compounds with more or less different quenching constants. It was shown that unlike individual QDs, the overall fluorescence response of the hybrid system allowed pattern-based discrimination of different samples of nitro-compounds. Afterward, we demonstrate that nanohybrid system can be used for simultaneous determination of 2,4,6-trinitrotoluene (TNT) and 4-nitrophenol. A calibration set including 36 samples in the concentration ranges of 2-30  $\mu\text{M}$  were used for building the PLS model and training the ANN. Accordingly, the average errors lower than 10 % were found in prediction of both analytes in the test set. However, nonlinear modeling (ANN) showed greater potential for quantitative analysis of the data investigated than the linear model (PLS). In order to investigate the feasibility of the simultaneous determination in a binary mixture at different selectivity and spectral overlapping cases, analysis of a series of simulated examples generated with two hypothetical fluorophores in the presence of two quenchers were considered and the results of PLS and ANN were compared.

## Introduction

During the past two decades, fluorescent quantum dots (QDs) have found notable interest in chemistry, physics, and biology for several reasons, including, high fluorescence quantum yield, size-controlled and shape-controlled absorption and luminescence features, narrow and symmetric emission bands, as well as their broad absorbance band.<sup>1-3</sup>

Since the photoluminescence (PL) of QDs arises from the recombination of the excitons (electrons and holes), it is expected that chemical or physical changes in the surrounding medium of QDs affect the efficiency of core electron-hole recombination and consequently the PL efficiency. Therefore, chemical sensing based on QDs can be developed using fluorescence changes induced by various strategies such as direct interaction of given chemical species with surface atoms or ligands of QDs, resonance energy transfer, and else.<sup>4</sup> Currently, QDs are being investigated as selective probes in aqueous samples. In general, the fluorescence intensity of QDs selectively responds to the presence of a desired analyte and therefore provides a general means for measuring the analyte concentration. Up to now, considerable progress in the application of QDs for optical sensing and biosensing has been

performed, either via PL quenching or enhancement. The improvements in this field are well reviewed everywhere.<sup>5-8</sup>

However, simultaneous determination of multiple analyt is a challenge for numerous chemical applications.<sup>9</sup> Achieving this goal with a focus on fluorescence-based probes has been a desired scope for researchers.<sup>10-14</sup> Regardless of the rare studies done in this area, they mostly rely on specific nucleic acid functionalized QDs that each nucleic acid sequence (or conjugated QD) selectively responds to a specific analyte.<sup>12, 15-17</sup> For example, R. Freeman et al.<sup>17</sup> modified two different sizes of CdSe/ZnS QDs with different nucleic acids exhibiting specific ion binding properties to selective detection of  $\text{Hg}^{2+}$  and  $\text{Ag}^+$ , the green-emitting QDs functionalized with the thymine-rich nucleic acid which selectively binds  $\text{Hg}^{2+}$  ions and the red-emitting QDs functionalized with the cytosine-rich nucleic acid which selectively binds  $\text{Ag}^+$  ions. A simple mixture of the both modified QDs was employed to simultaneous determination of the two ions. Wu et al.<sup>15</sup> developed an almost similar method, but using QDs labeled with different ion-specific DNazymes for multiplex detection of  $\text{Pb}^{2+}$  and  $\text{Cu}^{2+}$ . H. Kuang et al. simultaneously detected  $\text{Hg}^{2+}$  and  $\text{Ag}^+$  ions based on the fluorescence resonance energy transfer (FRET) between CdTe QD-DNA conjugates and dye-labeled single-strand DNA probes.<sup>16</sup>

In fact, the mentioned multiplex detection methods rely on two principles: first, each QD (or fluorophore) is selective to a specific analyte and second, the emission spectra of the QDs (or fluorophores) are well separated. W.J. Parak et al. reminded the problem of the spectral overlapping and suggested employing other resolution mechanisms such as distinguish based on the location of fluorophores<sup>18</sup>. They showed that the emission of two fluorophores, even with completely spectral overlapping, could be distinguished by confining them in separate containers, each bearing a different QD based barcode, and then read out in a single-particle manner. This method has been used to multiplexed sensing of  $H^+$ ,  $Na^+$ , and  $K^+$ .<sup>19</sup> The main drawbacks of this method are the limitation of the method to particles larger than the optical resolution limit ( $\geq 0.5 \mu m$ ) as well as difficulties in manufacturing of QD-barcode particles.

However, employing the selective probe for each analyst has been an essential part of the reported multiplexed sensing works. There are many examples that a favorite QD (or fluorophore) significantly response to more than one analyte and turned to be non-selective. In other word, beside this fact that the appropriate design of the QDs surface may, often, improve the selectivity of the systems, selectivity of many of the QDs (or fluorophore) is not as high as required to selective measurement.

Herein, we have employed a hybrid of carbon QDs (CQDs) and CdTe QDs as a nanohybrid system to show how non-selective QDs can be utilized to take useful advantages such as pattern-based discrimination of different analytes and even simultaneous determination in a binary mixture as well as comparing the quantitative results of linear and nonlinear multivariate chemometrics methods in handling the obtained data sets. Six nitro-compounds, which affect the fluorescence intensity of both QDs, were selected to check the performance of the nanohybrid system to achieve the proposed goals. The linear and nonlinear multivariate chemometrics methods such as partial least-squares (PLS) and artificial neural network (ANN) were used for simultaneous determination of the of 2,4,6-trinitrotoluene (TNT) and 4-nitrophenol (4-NP) based on the overall fluorescence of the nanohybrid system. In addition, the fluorescence data of two hypothetical fluorophores in the presence of two quencher at different selectivity and spectral overlapping cases were simulated according to a modified Stern-Volmer equation to show the ability of PLS and ANN to simultaneous quantitative analysis of data at different conditions and compare the results.

## Experimental section

### Reagents, apparatus and software

All chemicals were of analytical grade purity and used as received. Tellurium powder,  $CdCl_2 \cdot 5H_2O$ ,  $NaBH_4$ , L-cysteine, citric acid, and ethylenediamine, TNT, 2,4-dinitrotoluene (DNT), 4-NP, 2-nitrophenole (2-NP), 3-nitrotoaniline (3-NA) and, 4-nitrotoaniline (4-NA) were purchased from Sigma Aldrich (St. Louis, Mo, USA). Other routine chemicals were bought from Merck (Darmstadt, Germany). All solutions were prepared with double distilled water.

Fluorescence measurements were performed in a fast scanning mode of Varian Cary Eclipse spectrofluorometer equipped with a quartz cell (1 cm $\times$ 1 cm). Both excitation and emission slits were set to 5 nm. UV-Vis spectra were collected by an Agilent 8453 diode array spectrophotometer.

Calculations were performed in MATLAB 7.5.0 (The Mathworks, Natick, MA). The PLS analysis were carried out by means of the PLS Toolbox (Eigenvector Research, Inc., Manson, WA). The program codes written in our laboratory were used to process data, whenever necessary.

### Synthesis of Carbon QDs

The CQDs in this study were prepared by using the same procedures as those reported previously by B. Yang.<sup>20</sup> Briefly, CQDs were prepared as follows: 2g citric acid and 1 mL ethylenediamine were dissolved in 20 ml double distilled water and then transferred into a Teflon-lined stainless steel autoclave and heated in an oven at 180 ° C for 4 h. After this time, the autoclave was cooled to room temperature and CQDs were precipitated using acetone.

### Synthesis of CdTe QDs

The water-soluble CdTe QDs were synthesized according to the procedure reported in our previous work<sup>21</sup> with little modifications. In a typical synthesis, 0.1 mmol of  $CdCl_2 \cdot 5H_2O$  and 0.3 mmol of L-cysteine were mixed in 100 mL doubly distilled water in a three-necked flask to form the cadmium precursor. The pH of the solution was adjusted to 10 with 1M NaOH, and stirred under nitrogen purging for 30 min. Subsequently, the freshly prepared NaHTe (prepared by chemical reduction of tellurium powder with  $NaBH_4$ ) was injected into cadmium precursor under vigorous stirring to set the molar ratio of  $Cd^{2+}/Te/L-cys$  to 1/0.5/3. The solution placed into a Teflon-lined stainless steel autoclave and heated in an oven at 100 ° C for 3 h to obtain L-cysteine capped CdTe QDs.

### Measurement procedures

Appropriate amount of DNT, 4-NP, 2-NP, 3-NP and, 4-NP were dissolved in 10 mL of water/ethanol (4:1) solution and for TNT in the water/acetonitrile (4:1) solution to prepare 1mM stock solutions. A known concentration of each nitro-compound was added into the 2 mL of individual or hybrid of QDs solution (with pH 7.4, adjusted by Tris buffer solution (0.02 M)) and mixed thoroughly. The fluorescence spectrum of the solution was recorded in the range of 400–700 nm, with the excitation wavelength fixed at 340 nm. The concentrations of CQDs and CdTe QDs in the hybrid system were adjusted to such a value that exhibited equal fluorescence intensities. In the case of simultaneous determination, each measurement was an average of three replicates. All measurements were performed at room temperature and ambient conditions.

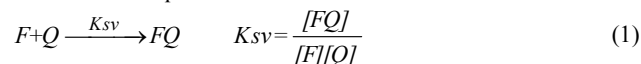
## Results and discussion

### Simulation

In order to illustrate how a hybrid of two fluorophores can discriminate different analytes and proving the capability of the hybrid system to simultaneous determination of analytes in a binary mixture, a series of simulated examples generated from two hypothetical fluorophores ( $F_1$  and  $F_2$ ) in the presence of two quenchers ( $Q_1$  and  $Q_2$ ) at different situations of selectivity and spectral overlapping were considered.

Generally, the dependence of the fluorescence intensity of the fluorophores upon quencher concentration is usually described by the Stern-Volmer equation (Eq. 2). In the case of static quenching (where a quencher interacts with the fluorophore in its ground state),

the following complex formation could be considered to drive the Stern-Volmer equation:<sup>22, 23</sup>



$$\frac{I_0}{I} = \frac{[F]_{tot}}{[F]} = \frac{[F]+[FQ]}{[F]} = 1 + K_{SV}[Q] \quad (2)$$

where  $[F]$  is the concentration of uncomplexed fluorophore,  $[Q]$  is the concentration of quencher,  $[FQ]$  is the concentration of the complex,  $K_{SV}$  is the Stern-Volmer constant for complex formation and,  $I_0$  and  $I$  are the fluorescence intensities observed in the absence and presence of quencher, respectively. Noted that according to this equation, the relationship between  $I_0/I$  and  $[Q]$  is linear with the slope of  $K_{SV}$ . In general, a more sensitive system will have a steeper slope and consequently a higher  $K_{SV}$  value. Therefore, the value of  $K_{SV}$  presents the sensitivity of the fluorophore toward the quencher. Noted that similar equation could be employed in the case of dynamic quenching. Subsequently, the change in the fluorescence intensity of the fluorophores in the presence of two quenchers may be described by the following equation:

$$\frac{I_0}{I} = \frac{[F]+[FQ_1]+[FQ_2]}{[F]} = 1 + K_{SV(F,Q_1)}[Q_1] + K_{SV(F,Q_2)}[Q_2] \quad (3)$$

where  $K_{SV(F,Q_1)}$  and  $K_{SV(F,Q_2)}$  are Stern-Volmer constants for complex formation of  $FQ_1$  and  $FQ_2$ , respectively. Here again  $I_0/I$  has a linear relationship with the concentration of  $Q_1$  and  $Q_2$ .

In this study three cases of the selectivity of fluorophores toward quenchers were simulated: case I) each fluorophore was 100% selective toward one quencher, case II) each fluorophore responds to both quenchers but more sensitive to one of them with the sensitivity ratio of 4:1, case III) similar to case II but with the sensitivity ratio of 4:3. The values of  $K_{SV}$  for all cases used to simulate data are listed in Table 1.

**Table 1** The Stern-Volmer values for three selectivity cases of two hypothetical fluorophores toward quenchers used in the simulated data.

		$Q_1$	$Q_2$
Case I)	$F_1$	2	0
	$F_2$	0	2
Case II)	$F_1$	2	0.5
	$F_2$	0.5	2
Case III)	$F_1$	2	1.5
	$F_2$	1.5	2

Two sets of fluorophores emission spectra with different peak centers were constructed using Gaussian peaks to simulate the situation where the emission spectra of fluorophores are well separated or have spectral overlapping (Fig. 1).

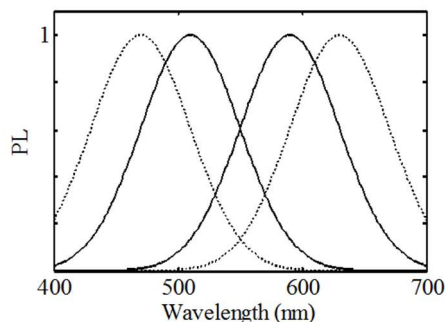


**Fig. 1** The emission spectra used in simulated data for two hypothetical fluorophores: separated spectra (dotted lines) and overlapped spectra (solid lines).

All three selectivity cases with both sets of fluorophore emission spectra were considered to simulate the related fluorescence data according to the equation (2) and (3). White noise with a standard deviation of 0.1% of the maximum values of data was added to all original simulated data sets.

As a specific case, let us consider case II of selectivity with spectral overlapping in the emission spectra of the fluorophores (see the written codes (M-file) in the supplementary information). Fig. 2 a and b show the fluorescence quenching of  $F_1$  in the presence of  $Q_1$  and  $Q_2$  at different concentrations (0-1), respectively. As it can be seen,  $Q_1$  and  $Q_2$  quench the  $F_1$  with different sensitivities (related to their  $K_{SV}$  values). Principal Component Analysis (PCA)<sup>24</sup> was applied over the column wised augmented fluorescence data sets in order to examine the ability of PCA to discriminate the samples related to each quencher. The result of PCA plot is shown in Fig. 2c. From the result, the first PC explains 98.7% of the data variance and the second PC only explains 0.1% of the data variance. This shows that almost all the variance of the augmented data set can be explained by just using the first PC and all other singular values explain the added random noise. In other word, rank of augmented data equals one, which means both quenchers influence the fluorescence of the  $F_1$  in the same pattern. As a result, it is not possible to discriminate  $Q_1$  and  $Q_2$  using this system. The same results can obtain for the fluorescence behavior of  $F_2$  in the present of the quenchers (Fig. 2d-f). In fact, this observation is expected and presence of any coexisting species that affects the fluorescence intensity of the fluorescent probe must be considered as an interference for the desired analyte.

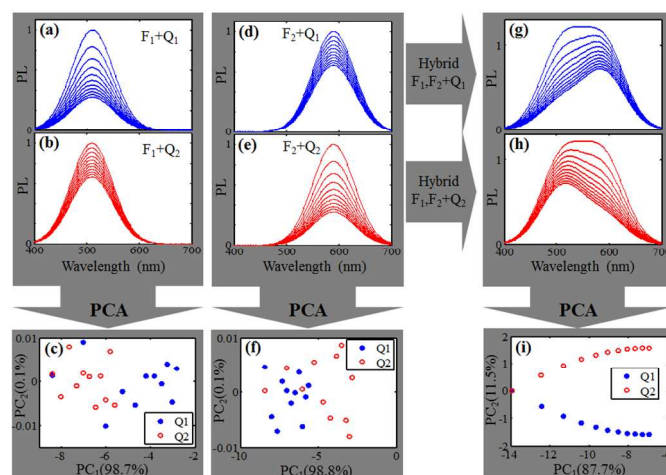


**Fig. 2** Fluorescence quenching of  $F_1$  (a and b),  $F_2$  (d and e) and, hybrid of  $F_1$ - $F_2$  (g and h) in the presence of  $Q_1$  and  $Q_2$ , respectively, and two-dimensional score plot of their augmented data sets (c, f and i).

Now, what if we mix both fluorophores making a hybrid system and record the overall fluorescence upon addition of each quencher. The fluorescence changes of the hybrid system in the presence of  $Q_1$  and  $Q_2$  are shown in Fig. 2g and h, respectively. The data sets were augmented and PCA was used to reduce the dimensionality of the augmented data set, again. Fig. 2i presents the PCA plot of the data set. It can be clearly seen that, in this case, there is a good separation between samples contain  $Q_1$  and those contain  $Q_2$ . Interestingly, for the hybrid system PC1 and PC2 explain 87.7% and 11.5% of the data variance, respectively. This means the rank of the data matrix is equal to two. This observation is because  $Q_1$  and  $Q_2$  could induce different quenching patterns in the overall fluorescence of the hybrid system. This observation could be considered as an evidence that the

hybrid system may have the capability to simultaneous determination of the quenchers.

To examine this possibility, both linear and non-linear multivariate calibration methods such as PLS<sup>25, 26</sup> and back propagation ANN (BP-ANN)<sup>27, 28</sup> were used for simultaneous determination of quenchers. The PLS method generally presumes that there is a linear relationship between response and analyte concentrations. However, in many cases Stern-Volmer plots tend to deviate from linearity (for example, at higher concentrations of quencher or by the simultaneous appearance of static and dynamic quenching). On the other hand, BP-ANN model is able to handle both linear and nonlinear relationships well. A full factorial design was used to obtain 36 samples for the calibration set at six concentrations of each quencher (0, 0.2, 0.4, 0.6, 0.8, and 1) and 9 samples for the test set at three concentration levels (0.1, 0.3, and 0.5). The data sets were built for all three selectivity cases with both emission spectra sets. As previously, a random noise with the standard deviation of 0.1% of data maximum value was added to the original data. The relative fluorescence data ( $I_0/I$ ) and the original fluorescence data ( $I$ ) were selected as appropriate responses for PLS and BP-ANN, respectively. Noted that  $I$  is not linear with the concentration of the quenchers. In the case of PLS model, both fluorescence data and concentration vectors were employed after a mean centering as preprocessing. The first two significant PCs of data sets were normalized as the input to train the ANN and a model with two hidden layers, each contains four nodes, was selected. The overall performance of the models was evaluated in terms of RMSE (root mean square error) in the prediction of  $Q_1$  and  $Q_2$  concentrations in the test set. The calculated RMSE values for each calibration method are listed in Table 2.

**Table 2** The RMSE values in the prediction of  $Q_1$  and  $Q_2$  concentrations in the test set using PLS and BP-ANN.

	RMSE ( $\times 10^{-3}$ )	
	PLS	BP-ANN
Case I with spectral overlapping	2.51	0.28
Case I with separated spectra	0.34	0.67
Case II with spectral overlapping	3.25	0.73
Case II with separated spectra	0.36	1.29
Case III with spectral overlapping	5.25	2.28
Case III with separated spectra	1.43	1.70

As can be seen, despite the small differences between the results, both PLS and BP-ANN models were successfully able to predict concentrations of both quenchers with acceptable RMSE values. These observations proved the ability of the multivariate Chemometrics methods for simultaneous determination of analytes base on the fluorescence of a hybrid of even non-selective fluorophores. However, BP-ANN gave better results than the PLS method for data sets with spectral overlapping. In contrast, the PLS model produced better results for data sets simulated with separated spectra. In general, using more selective fluorophores in the hybrid system result in lower RMSE values in the prediction of the test set. It should be noted that where the value of  $(K_{sv(F_1, Q_1)}/K_{sv(F_2, Q_1)})$  be equal to  $(K_{sv(F_1, Q_2)}/K_{sv(F_2, Q_2)})$  Or where the emission spectra of fluorophores are completely overlapped, rank of the data matrix remains equal to one and consequently, both quenchers make the

same pattern and their simultaneous determination could not be achieved.

### Optical properties of synthesized quantum dots

UV-Vis and emission spectra of as-prepared CQDs and CdTe QDs are shown in Fig. 3a. It can be seen that the prepared CQDs possess UV-vis absorption spectrum with a peak at 340 nm and an emission band ranging from 400 to 550 nm with the maximal fluorescence wavelength at 450 nm. The prepared CdTe QDs show a broad UV absorption and excitation spectra with an emission spectrum at about 590 nm. The emission spectra of both CQDs and CdTe QDs have almost the same full width at half maximum (FWHM) of around 70 nm.

In general, QDs are characterized by their broad absorbance bands and thus multicolor QDs can be simultaneously excited by a single excitation source. This advantage makes QDs much more favorable to achieve multiplexed detection than conventional organic fluorophores that require the excitation light source be tuned into their respective narrow absorption bands.<sup>2, 12, 29</sup> Thoroughly mixing of the CQDs and CdTe QDs in aqueous solution produce a nanohybrid system displayed an overall fluorescence with two emission peaks centered around 440 nm for CQDs and 590 nm for CdTe QDs under excitation at 340 nm. The hybridization occurs through interactions of hydrogen bonding and electrostatic attraction between the QDs.<sup>30</sup> Fluorescence spectra of the nanohybrid system solution containing a fixed amount of CQDs and different concentrations of CdTe QDs are shown in Fig. 3b. The ratios of fluorescence intensities at 440 and 590 nm could be easily tuned by using different amounts of QDs.

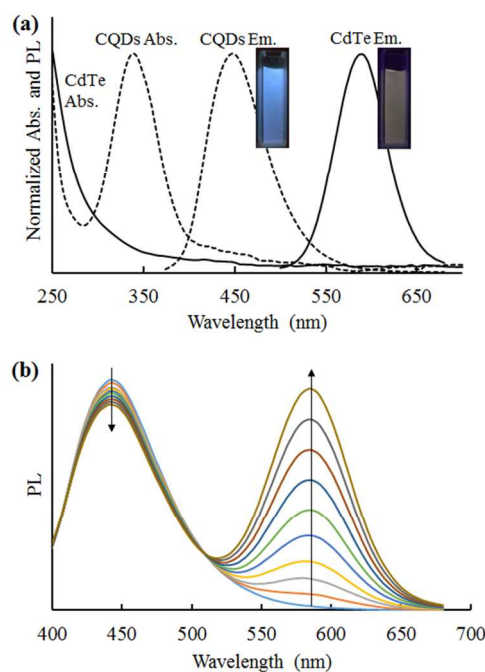


**Fig. 3.** (a) Normalized UV-vis absorption and emission spectra of CdTe QDs (solid lines) and CQDs (dash lines). Insets show the photographs of QDs dispersion in water with UV (365 nm) illumination. (b) the overall Fluorescence spectra of the nanohybrid system at a fixed amount of CQDs upon the addition of different concentrations of CdTe QDs.

## pattern-based discrimination and Simultaneous determination

To illustrate the reliability of the method, CQDs and CdTe QDs were considered to produce a nanohybrid system and utilize as the fluorescent probe and some nitro-compounds such as TNT, DNT, 4-NP, 2-NP, 4-NA and 3-NA which were able to quench both QDs were also considered as quenchers. First, to evaluate the capability of the QDs for quantitative detection of nitro-compounds, the fluorescence intensity of QDs in response to the increasing concentration of each nitro-compound (0–100  $\mu\text{M}$ ) were monitored. The strong fluorescence quenching for

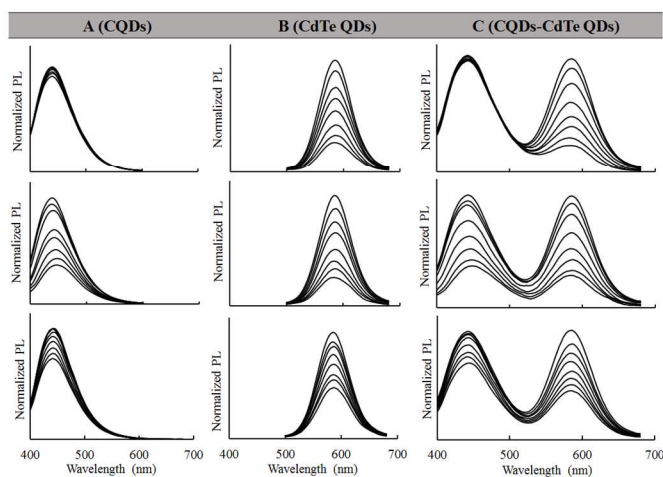


Fig. 4. Fluorescence quenching of CQDs (column A), CdTe QDs (column B) and, hybrid of CQDs-CdTe QDs (column C) in the presence of different concentrations (0, 2, 6, 20, 40, 60, 80 and, 100  $\mu\text{M}$ ) of TNT, 4-NP and, 3-NA from up to down, respectively.

CQDs was observed in the presence of 4-NP and 4-NA while TNT and DNT had relatively weak effects on the fluorescence intensity. In contrast, CdTe QDs showed the highest sensitivity toward TNT, DNT and, 4-NP. As an example, the fluorescence quenching of CQDs and CdTe QDs with the addition of TNT, 4-NP and, 3-NA are shown in Fig. 4 columns A and B, respectively. It should be noted that all fluorescence data well followed the Stern–Volmer equation (Table S1).

According to the previous works, quenching of the CdTe QDs with nitro-compounds can be attributed to the formation of Meisenheimer complex formed between nitro-compounds and primary amino groups on the surface of the QDs. Subsequently, a strong charge-transfer interaction occurs between the electron deficient aromatic ring of nitro-compounds and the electron-rich amino groups, resulting in decreasing the fluorescence intensity.<sup>31</sup> On the other hand, photoexcited CQDs have been proposed as both electron donors and electron acceptors and quenching their luminescence emission intensities by two nitro-compounds including 4-nitrotoluene and DNT were attributed to the electron accepting efficiency of the nitro-compounds.<sup>32</sup> However, the energy transfer from excited CQDs to nitro-compounds caused by the overlapping between the emission

spectrum of CQDs and UV-Vis absorption of nitro-compounds can better explain the observed quenching efficiencies of nitro-compounds (Fig. S1).

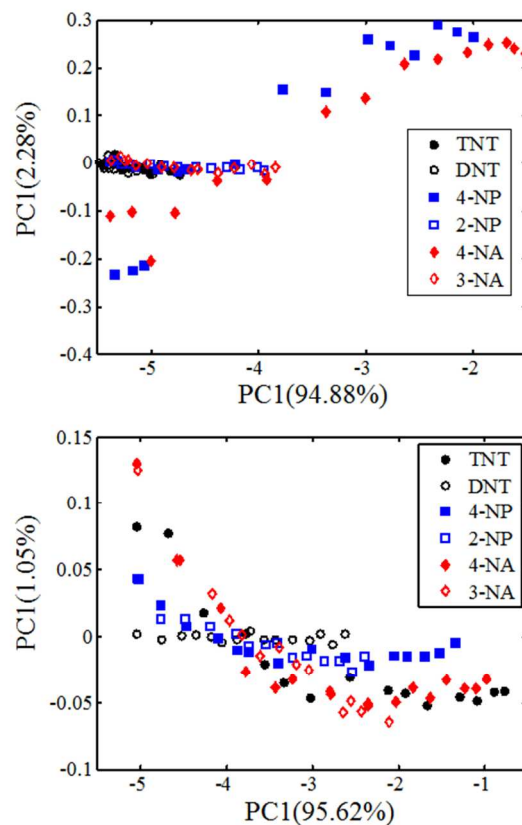


Fig. 5. Plot of first two principal component for augmented fluorescence data set of CQDs (a) and CdTe QDs (b) with the addition of different nitro-compounds.

In the following, to demonstrate if different nitro-compounds can be discriminated using the fluorescence quenching of individual or a hybrid of QDs, first, data sets obtain from treating of each QD with nitro-compounds were augmented and analyzed with PCA (Fig. 5). For the CQDs data set, the first and second PCs explain 94.88% and 2.28% of the total variance, respectively, and for the CdTe data set these values are equal to 95.62% and 1.05%, respectively. In fact, the percentage of variance explained by the second PC for CQDs data set is greater than the corresponding value of the CdTe QDs data set. In addition, for this data set, two of the nitro-compounds (4-NP and 4-NA) show a relatively different pattern than other nitro-compounds. These differences mostly arise from a few wavelength blue-shift of the CQDs fluorescence peak position during the addition of these two compounds. However, as was expected, the second PCs just explain a slight percentage of the total variance and no real discrimination between the Nitro-compounds were observed.

Subsequently, the nitro-compounds were treated at the same concentration ranges with the hybrid of two QDs. The fluorescence response of the nanohybrid system to TNT, 4-NP and, 3-NA, are shown in Fig. 4 columns C. As can be seen, the

overall fluorescence quenching of the nanohybrid responses to the nitro-compounds could be significantly different. The whole fluorescence data sets were augmented and the efficacy of PCA was applied on the augmented data set. The result of PCA plot is shown in a two-dimensional score plot (Fig. 6). As shown, the first two principal components explain 85.62% (PC1) and 9.58% (PC2) of the total variance within the data set. This is obvious that samples for different nitro-compounds (with the exception of TNT and DNT) appear along the separated curves. This is indicative of this fact that different Nitro-compounds can produce distinct patterns in the fluorescence quenching that are diagnostic for the presence of that particular compound.

Having these primary results and based on the concept demonstrated in the previous part, we turn to simultaneous determination by using this nanohybrid system and applying multivariate chemometrics methods. It is clear that using this nanohybrid system and the explained procedure, no more than two components could be determined simultaneously. Thus, TNT and 4-NP were nominated to produce a binary mixture and evaluate the possibility of their simultaneous determination. A set of 36 calibration samples for six concentration values of

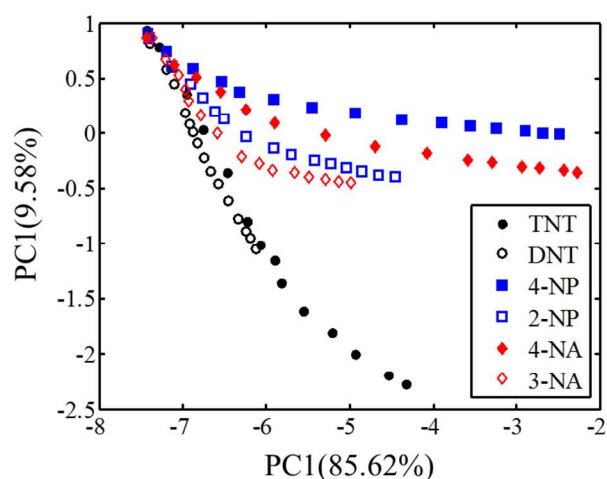


**Fig. 6** Plot of first two principal component for augmented fluorescence data set of the nanohybrid of CQDs-CdTe QDs with the addition of different nitro-compounds.

TNT and 4-NP (2, 5, 7, 10, 20 and, 30  $\mu\text{M}$ ) were used to obtain the regression models (Table 3).

As a multivariate linear calibration method, PLS regression was considered to use the complete range of fluorescence spectra. Both  $X$  matrix ( $I_0/I$ ) and  $y$  vectors (concentrations of TNT or 4-NP) were mean-centered and PLS calibration carried out using PLS-1. The number of latent variables was optimized with the target of obtaining a minimal root-mean square error of cross validation (RMSECV). In addition, as a nonlinear calibration method, the feed-forward neural network that was trained by back-propagation algorithm was also used. The input layer contained the normalized two first PCs of the calibration data set ( $I$ ) and, the outputs were natural logarithm of TNT and 4-NP concentrations. The selection of the right number of hidden layers and optimum number of each hidden layer's

nodes were performed according to the minimum value of RMSECV. Therefore, a BP-ANN with two hidden layers contain two nodes in each hidden layer was used.

**Table 3** Actual and corresponding observed PLS and ANN predicted values for TNT and 4-NP

Samples	Actual concentrations ( $\mu\text{M}$ )		PLS		BP-ANN	
	TNT	4-NP	TNT	4-NP	TNT	4-NP
<b>Calibration (Training) set</b>						
1	2	2	1.64	3.78	2.15	1.80
2	2	5	2.22	6.90	2.58	5.46
3	2	7	2.12	6.52	2.94	6.50
4	2	10	-0.05	13.20	2.05	9.79
5	2	20	-0.40	17.32	2.27	18.86
6	2	30	-1.12	27.33	2.04	33.19
7	5	2	2.60	3.64	2.87	2.08
8	5	5	7.51	4.92	4.64	4.91
9	5	7	4.98	6.59	5.01	7.57
10	5	10	5.70	10.40	4.92	8.93
11	5	20	6.19	18.22	5.05	19.87
12	5	30	4.18	25.98	4.21	30.65
13	7	2	8.07	3.16	5.64	2.02
14	7	5	9.11	4.41	7.36	5.15
15	7	7	8.76	4.43	6.66	7.87
16	7	10	6.00	12.83	6.03	10.45
17	7	20	7.57	18.66	6.13	19.82
18	7	30	7.99	26.49	8.19	27.21
19	10	2	13.80	-0.26	12.05	1.76
20	10	5	14.03	3.69	11.20	4.42
21	10	7	11.21	6.18	12.32	7.62
22	10	10	11.13	13.50	9.74	11.31
23	10	20	9.24	24.49	10.68	23.44
24	10	30	9.11	33.80	9.15	29.23
25	20	2	18.18	2.78	17.43	2.33
26	20	5	18.04	4.28	18.27	5.19
27	20	7	24.00	5.43	21.18	5.09
18	20	10	21.03	8.09	24.22	8.59
29	20	20	26.78	22.32	22.24	19.58
30	20	30	23.64	29.34	22.27	27.34
31	30	2	24.76	3.54	25.07	2.52
32	30	5	24.57	4.73	27.34	4.95
33	30	7	29.16	5.88	32.36	7.98
34	30	10	26.39	10.11	27.77	9.36
35	30	20	27.64	20.84	28.91	21.25
36	30	30	31.37	30.07	26.80	28.22
<b>Average error</b>			<b>26.4%</b>	<b>24.7%</b>	<b>12.3%</b>	<b>8.4%</b>
<b>Test set</b>						
1	5	15	5.7	13.8	4.8	12.3
2	10	15	11.0	17.8	10.0	17.6
3	10	25	8.5	27.7	9.2	27.8
4	15	5	15.7	4.7	14.5	4.9
5	15	10	17.5	11.0	16.8	9.2
6	15	15	15.2	17.6	14.5	16.3
7	15	25	14.3	26.0	14.5	25.8
8	25	15	24.3	14.8	25.3	13.5
9	25	25	22.5	26.5	22.9	26.4
10	15	30	18.0	29.1	18.5	27.3
<b>Average error</b>			<b>9.9%</b>	<b>8.5%</b>	<b>6.7%</b>	<b>9.3%</b>

The predicted results by PLS (with three latent variables) and BP-ANN models for calibration (training) set are shown in Table 3. The PLS model had average errors of 26.4% and 24.7% for TNT and 4-NP, respectively, while for BP-ANN these values were equal to 12.3% and 8.4%. Obviously, considering the whole range of concentrations, BP-ANN gives

much better results than PLS model. However, the highest values of prediction error pertain to prediction of lower concentrations (mainly for PLS model). Both BP-ANN and PLS models have much more acceptable predictions for higher concentrations. Noted that excluding the concentrations equal to 2  $\mu\text{M}$  will drop the average errors for the PLS model significantly.

In order to evaluate the accuracy of the regression models, the concentrations of TNT and 4-NP in 10 test samples (not included in the calibration set) were estimated (Table 3). The average errors, lower than 10 % were found in prediction of both nitro-compounds by applying the PLS calibration model and trained ANN. Several different approaches for determination of the detection limit (DL) in the multivariate calibration methods have been reported.<sup>33,34</sup> In the case of PLS regression, the approach provided by Ubide et al.<sup>35</sup> which is an extension of IUPAC recommendations for univariate calibration to multivariate calibration was used. Following the proposed approach, once the optimum number of latent variables is selected, calculation of DL can be achieved by:

$$\hat{C}_{DL} = \mathbf{x}_{blank} \cdot \mathbf{b} + 3 \cdot s_{blank} \cdot \mathbf{b} \quad (1)$$

where  $\mathbf{x}_{blank}$  and  $s_{blank}$  are the signal vector and the standard deviation vector of blank (Fluorescence of hybrid system in the absence of quenchers), respectively, and  $\mathbf{b}$  is the regression vector.  $s_{blank}$  can be estimated from  $n$  measurements of the blank solution.

Finally, for the PLS regression the DL of 1.34 and 3.16  $\mu\text{M}$  for TNT and 4-NP were determined, respectively. In a similar manner,  $\mathbf{x}_{blank} + 3 \times s_{blank}$  was also introduced to the ANN and the DL of 2.01  $\mu\text{M}$  for TNT and 1.88  $\mu\text{M}$  for 4-NP was obtained.

## Conclusions

In summary, the applications of both linear and nonlinear multivariate calibration methods for simultaneous determination of analytes in a binary mixture base on the overall fluorescence of a nanohybrid system comprises two non-selective QDs (CQDs and CdTe QDs) were introduced and compared. The results were relatively successful, although they were not completely satisfactory. It was shown that ANN has greater potential than PLS to deal with the problem that was analyzed in this paper.

This study could be considered as an opening to overcome some limitations of traditional intensity based fluorescence sensing that limit the application of non-selective fluorophores to quantitative analyses in solution. In this case, the only requirement is that the selectivity ratio of the first fluorophore toward analytes (for example the ratio of Stern-Volmer constants) be different from the according value for the second fluorophore. It should be noted that this strategy would not be limited to applying a hybrid of two fluorophores. Even only one kind of fluorophore but at different experimental conditions which are able to change the selectivity of the fluorophore

toward analytes might produce the opportunity to simultaneous determination.

## Notes and references

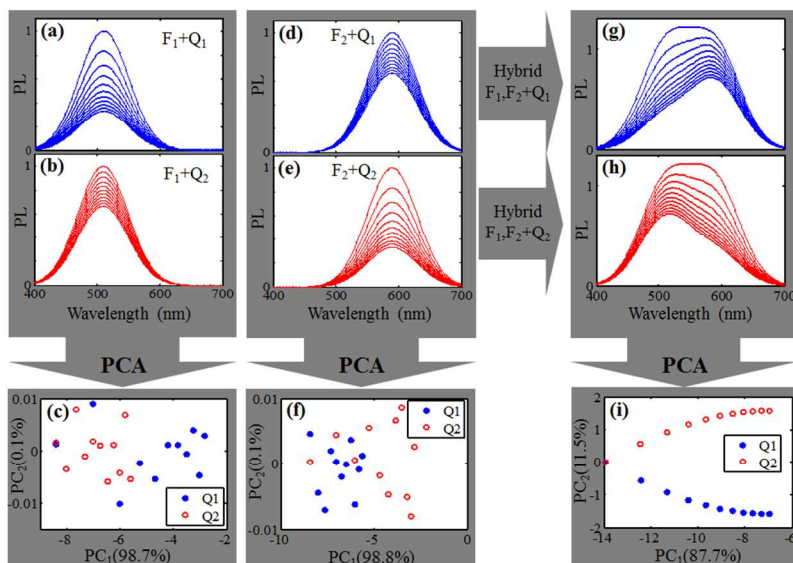
<sup>a</sup> Faculty of Chemistry, Institute for Advanced Studies in Basic Sciences, Zanjan, Iran. Corresponding Author Hamid Abdollahi, Fax: +982414153232; Tel: +982414153122; E-mail: [abd@iasbs.ac.ir](mailto:abd@iasbs.ac.ir); [ali\\_barati@iasbs.ac.ir](mailto:ali_barati@iasbs.ac.ir).

<sup>b</sup> Department of Chemistry, Razi University, Kermanshah, Iran. E-mail: [mshamsipur@yahoo.com](mailto:mshamsipur@yahoo.com)

Electronic Supplementary Information (ESI) available: See DOI: 10.1039/b000000x/

- R.C. Somers, M.G. Bawendi, D.G. Nocera, *Chem. Soc. Rev.*, 2007, **36**, 579-591.
- D.M. Willard, A. Van Orden, *Nat. Mater.*, 2003, **2**, 575-576.
- R. Gill, M. Zayats, I. Willner, *Angew. Chem., Int. Ed.*, 2008, **47**, 7602-7625.
- M.J. Ruedas-Rama, E.A. Hall, *Analyst*, 2009, **134**, 159-169.
- R. Freeman, I. Willner, *Chem. Soc. Rev.*, 2012, **41**, 4067-4085.
- D. Jimenez de Aberasturi, J.-M. Montenegro, I. Ruiz de Larramendi, T.f. Rojo, T.A. Klar, R. Alvarez-Puebla, L.M. Liz-Marzán, W.J. Parak, *Chem. Mater.*, 2012, **24**, 738-745.
- P. Wu, T. Zhao, S. Wang, X. Hou, *Nanoscale*, 2014, **6**, 43-64.
- Y. Lou, Y. Zhao, J. Chen, J.-J. Zhu, *J. Mater. Chem. C*, 2014, **2**, 595-613.
- N. Singh, R.C. Mulrooney, N. Kaur, J.F. Callan, *Chem. Commun.*, 2008, 4900-4902.
- W.C. Chan, D.J. Maxwell, X. Gao, R.E. Bailey, M. Han, S. Nie, *Curr. Opin. Chem. Biol.*, 2002, **13**, 40-46.
- S. Nagl, O.S. Wolfbeis, *Analyst*, 2007, **132**, 507-511.
- M. Han, X. Gao, J.Z. Su, S. Nie, *Nat. Biotechnol.*, 2001, **19**, 631-635.
- M.J. Ruedas-Rama, X. Wang, E.A. Hall, *Chem. Commun.*, 2007, 1544.
- S. Carregal-Romero, E. Caballero-Díaz, L. Beqa, A.M. Abdelmonem, M. Ochs, D. Hühn, B.S. Suau, M. Valcarcel, W.J. Parak, *Annu. rev. anal. chem.*, 2013, **6**, 53-81.
- C.-S. Wu, M.K. Khaing Oo, X. Fan, *ACS Nano*, 2010, **4**, 5897-5904.
- C. Hao, L. Xua, C. Xing, H. Kuang, L. Wang, C. Xu, *Biosens. Bioelectron.*, 2012, **36**, 174-178.
- R. Freeman, T. FINDER, I. Willner, *Angew. Chem., Int. Ed.*, 2009, **48**, 7818-7821.
- A.Z. Abbasi, F. Amin, T. Niebling, S. Friede, M. Ochs, S. Carregal-Romero, J.-M. Montenegro, P. Rivera Gil, W. Heimbrot, W.J. Parak, *ACS Nano*, 2011, **5**, 21-25.
- L.L. del Mercato, A.Z. Abbasi, M. Ochs, W.J. Parak, *ACS Nano*, 2011, **5**, 9668-9674.
- S. Zhu, Q. Meng, L. Wang, J. Zhang, Y. Song, H. Jin, K. Zhang, H. Sun, H. Wang, B. Yang, *Angew. Chem., Int. Ed.*, 2013, **125**, 4045-4049.
- M. Shanehsaz, A. Mohsenifar, S. Hasannia, N. Pirooznia, Y. Samaei, M. Shamsipur, *Microchim. Acta*, 2013, **180**, 195-202.

- 1  
2  
3  
4  
5  
6  
7  
8  
9  
10  
11  
12  
13  
14  
15  
16  
17  
18  
19  
20  
21  
22  
23  
24  
25  
26  
27  
28  
29  
30  
31  
32  
33  
34  
35  
36  
37  
38  
39  
40  
41  
42  
43  
44  
45  
46  
47  
48  
49  
50  
51  
52  
53  
54  
55  
56  
57  
58  
59  
60
- 22 J.R. Lakowicz, Principles of fluorescence spectroscopy, Springer, 3rd edn., 2007, ch. 8, pp. 278-283.
- 23 I. Oehme, O.S. Wolfbeis, *Microchim. Acta*, 126 (1997) 177-192.
- 24 H. Abdi, L.J. Williams, *Wiley Interdiscip. Rev. Comput. Stat.*, 2010, **2**, 433-459.
- 25 T.F. Cullen, S.R. Crouch, *Microchim. Acta*, 1997, **126**, 1-9.
- 26 D.M. Haaland, E.V. Thomas, *Anal. Chem.*, 1988, **60**, 1193-1202.
- 27 J.R. Long, V.G. Gregoriou, P.J. Gemperline, *Anal. Chem.*, 1990, **62**, 1791-1797.
- 28 L. Hadjiiski, P. Geladi, P. Hopke, *Chemom. Intell. Lab. Syst.*, 1999, **49**, 91-103.
- 29 S. Hohng, T. Ha, *ChemPhysChem*, 2005, **6**, 956-960.
- 30 H. Zhu, W. Zhang, K. Zhang, S. Wang, *Nanotechnology*, 2012, **23**, 315502.
- 31 S. Xu, H. Lu, J. Li, X. Song, A. Wang, L. Chen, S. Han, *ACS Appl. Mater. Interfaces*, 2013, **5**, 8146-8154.
- 32 X. Wang, L. Cao, F. Lu, M.J. Meziani, H. Li, G. Qi, B. Zhou, B.A. Harruff, F. Kermarrec, Y.-P. Sun, *Chem. Commun.*, 2009, 3774-3776.
- 33 M. Ortiz, L. Sarabia, A. Herrero, M. Sanchez, M. Sanz, M. Rueda, D. Gimenez, M. Melendez, *Chemom. Intell. Lab. Syst.*, 2003, **69**, 21-33.
- 34 M. Rodriguez-Cuesta, R. Boque, F. Xavier Rius, *Anal. Chim. Acta*, 2003, **476**, 111-122.
- 35 M. Ostra, C. Ubide, M. Vidal, J. Zuriarrain, *Analyst*, 2008, **133**, 532-539.



The overall fluorescence of a hybrid of two non-selective quantum dots (CQDs and CdTe QDs) has been used to pattern-based discrimination of different analytes and simultaneous determination in a binary mixture of analytes.